*Macromolecules* **2007,** *40,* 5526−5536

# Microstructures Formed in Co-Cross-Linked Networks and Their Relationships to the Optical and Mechanical Properties of PNIPA/Clay Nanocomposite Gels

**Kazutoshi Haraguchi*,[†] and Liyuan Song[‡]**

*Material Chemistry Laboratory, Kawamura Institute of Chemical Research, 631 Sakado, Sakura, Chiba 285-0078, Japan, and College of Material Science & Engineering, Donghua University, Shanghai 200051, China*

*Received March 22, 2007*

ABSTRACT: PNIPA/clay nanocompoiste gels with co-cross-linked networks were synthesized by in-situ, free-radical polymerization of NIPA (*N*-isopropylacrylmaide) in the presence of two types of cross-linker, an inorganic cross-linker (clay: hectorite) and an organic cross-linker (*N*,*N*′-methylenebis(acrylamide): BIS), with concentrations *n* and *m*, respectively, in aqueous media. The optical properties and the tensile and compressive mechanical properties of the resulting hydrogels (NC*n*−OR*m* gels) were investigated and are discussed herein in terms of co-cross-linked PNIPA network structures. NC*n*−OR*m* gels were all uniform, but their transparencies changed considerably according to *n* and *m* and were generally different from the sum of the transparencies of corresponding NC*n* and OR*m* gels. NC*n*−OR*m* gels generally exhibited pronounced weakness and brittleness in tensile tests, like OR*m* gels. In contrast, in compressive mechanical tests, large improvements were achieved at high *n* and low *m* values ($m \leq 1$: e.g., NC5−OR0.3). Furthermore, abnormal increases in modulus were observed in both mechanical tests. All of these results are explained by the formation of a "microcomplex structure" consisting of exfoliated clay platelets and PNIPA chains with enhanced chemical cross-linking. The mechanism of forming the proposed microcomplex structure is discussed and is based on a preferential distribution of BIS to clay in the reaction solution and the formation of clay−brush particles during synthesis.

## Introduction

Polymeric hydrogels, which are soft, wet materials composed of a hydrophilic polymer network and a large amount of water, exhibit many outstanding characteristics which are distinct from those of solid materials: high water absorption, high diffusion rate for solutes, soft mechanical properties, wet surfaces, high transparency, good biocompatibility, and so on. Especially in the past two decades, polymeric hydrogels consisting of poly(*N*-isopropylacrylamide) (PNIPA) have drawn considerable attention as promising advanced functional materials because of their well-defined stimuli sensitivities at the lower critical solution temperature (LCST) in terms of gel volume, surface property (hydrophilic−hydrophobic changes), optical transparency (transparent−opaque), and the adsorption/desorption of solutes.[1−5] However, so far, conventional PNIPA hydrogels (abbreviated to OR gels) prepared using an organic cross-linker or an irradiation by $\gamma$-rays have shown serious disadvantages in terms of their mechanical, structural, and absorption properties due to their chemically cross-linked networks. Constant efforts have been made to improve the very poor mechanical properties of OR gels as well as their limited functional properties such as the low degree of swelling, the slow deswelling rate, and the erratic release of solutes.[6−12] In order to mitigate their mechanical fragility, OR gels have been modified using inorganic components, such as in-situ polymerized silica,[6] inorganic clay,[7] and organically modified clays,[8] together with the organic cross-linker. However, in all cases, the poor mechanical properties were hardly improved by the incorporation of these inorganic nanoparticles. This is mainly due to the predominant role of chemically cross-linked networks in the destruction of the hydrogels by external forces; i.e., the coexisting inorganic nanoparticles do not act as effective reinforcing agents in toughening these chemically cross-linked hydrogels.

Recently, it was found that the mechanical properties of PNIPA hydrogels were dramatically improved by using exfoliated clay nanoparticles instead of organic cross-linkers.[13] That is, a new type of hydrogel (referred to as "nanocomposite hydrogels" or "NC gels"), synthesized by the in-situ, free-radical polymerization of a monomer (e.g., NIPA) in the presence of exfoliated inorganic clay (e.g., hectorite) in aqueous media, can overcome all of these mechanical and functional disadvantages. NC gels exhibited extraordinary good mechanical properties, such as ultrahigh elongation at break (ca. 1000%), high fracture energy (up to 3300 times that of OR gels), modulus and strength which could be controlled over a wide range depending on the clay concentration, and superb swelling and deswelling properties.[14−16] All of these characteristics were attributed to the organic/inorganic networks formed in the NC gels, which consist of exfoliated clay platelets uniformly dispersed in an aqueous medium with a number of flexible polymer chains linking them together.[17] In this structure, the clay platelets act as a super-multifunctional cross-linking agent which enables PNIPA to form effective planes of (physical) cross-links.[18−20] In contrast, conventional OR gels as well as the silica- or clay-containing OR gels described above exhibit only weakness and brittleness, regardless of the concentrations of the organic cross-linker[13−16] and the silica or clay.[6−8] Thus, it was concluded that NC gels cross-linked by exfoliated inorganic clay platelets have extraordinarily high mechanical toughness.

However, so far, as shown in Figure 10 (NC gels) of the present paper, the mechanical properties achieved in NC gels

---

* To whom correspondence should be addressed: e-mail hara@kicr.or.jp; Tel +81-43-498-2111; Fax +81-43-498-2182.

[†] Kawamura Institute of Chemical Research.

[‡] Donghua University.

10.1021/ma070695p CCC: $37.00

with a constant polymer/water ratio (1 M of PNIPA) were limited to a small range in terms of the modulus−strength relationship. That is, the modulus and strength could be changed in a linear fashion by altering the cross-linker (clay) concentration. In order to control the mechanical properties of the NC gels over a broad range, the organic/inorganic network structure, which is the chief determining factor of the superior properties described above, must be modified in a different manner. Here, we focus on the modification of the network by means of chemical cross-links (covalent bonds) introduced into the organic (PNIPA)/inorganic (clay) network.

As for the coexistence of clay nanoparticles and chemical cross-links in the hydrogel, only limited effects on the swelling and deswelling, such as the lowering of the LCST behavior in the case of inorganic clay[7] and the enhancement of the temperature response in the case of organically modified clay,[8] have been reported. So far, there have been no reports on changes in the mechanical properties and structural homogenity (transparency) of chemically cross-linked PNIPA/clay gel systems. This is probably due to the fact that no one has been able to make any remarkable improvements to the system. On the other hand, interesting characteristics (e.g., high strength and low bulk density) in nanocomposites (solids) consisting of chemical cross-links and inorganic materials have been reported recently, although systems, such as PNIPA/clay aerogel composites,[21] prepared using spongy clay and an organic cross-linker, and chemically cross-linked silica aerogels,[22] are totally different from the present hydrogel. In the present study, we investigated the precise effects of chemical cross-links coexisiting in an organic/inorganic network on the optical and mechanical properties of NC gels and found unusually large changes in the optical properties and the tensile and compressive mechanical properties by forming a microcomplex structure consisting of chemical cross-links and exfoliated clay.

## Experimental Section

**Synthesis.** Co-cross-linked NC gels were prepared using different amounts of organic cross-linker (BIS) along with inorganic clay (hectorite: Laponite XLG: Lockwood, Ltd., UK). The resulting hydrogels were named NC*n*−OR*m* gels, according to the amounts of inorganic clay (*n* mol % per L of $H_2O$) and BIS (*m* mol % against the NIPA monomer), while the monomer (NIPA) and water were fixed at 1 mol per L of $H_2O$ and 30 mL of $H_2O$, respectively. Except for the use of BIS, the synthesis procedure was the same as that reported previously.[16,17] For example, to prepare the NC5−OR0.5 gel, an aqueous solution consisting of water (28.5 mL), inorganic clay (1.143 g), NIPA (3.39 g), and BIS (0.021 g) was prepared, followed by the addition of the catalyst (*N*,*N*,*N*′,*N*′-tetramethylethylenediamine: TEMED, 24 $\mu$L) and an aqueous solution of the initiator (potassium peroxodisulfate: KPS, 0.03 g in 1.5 mL of $H_2O$). Transparent initial reaction solutions for the NC−OR gels were prepared at ice−water temperature. Then, free-radical polymerization was allowed to proceed in a water bath at 20 °C for 20 h. In this study, the amounts of clay and BIS were varied over the ranges of 1−10 mol % per L of $H_2O$ (NC1 to NC10) and 0.02−5 mol % with respect to NIPA (OR0.02 to OR5), respectively. Throughout all experiments, oxygen was excluded from the system. All NC−OR gels were synthesized in two kinds of vessels: a tubular glass vessel (interior size: 5.5 mm diameter × 200 mm length) and a polystyrene cuvette (10 × 10 × 44 mm length) with cap for optical use.

**Measurements.** *Transparency*. The transparencies were measured at 600 nm using a UV/vis spectrophotometer (V-530, JASCO Co., Japan) for all gels (as-prepared NC, OR, and NC−OR gels) in a cubic polystyrene cuvette at 20 °C.

*Transmission Electron Microscopy (TEM)*. TEM was undertaken using a JEM-2200FS (Nihon Denshi Co.) instrument at 200 kV for dried NC−OR gels. Ultrathin films (ca. 70 nm thick) were prepared for TEM observation by cutting the dried gels embedded in epoxy resin using an ultra-microtome (Reichert Ultracut S).

*X-ray Diffraction (XRD)*. XRD profiles were obtained using milled, dried samples under Cu−Kα X-ray irradiation on a Rigaku-Denki RX-7 diffractometer. As an internal reference, a small amount of silicon metal was used by incorporating it into the sample.

*Mechanical Properties*. Tensile measurements were performed on as-prepared NC, OR, and NC−OR gel samples of the same size (5.5 mm diameter × 70 mm length) using a Shimadzu Autograph AGS-H. The tensile properties of the NC gels were obtained under the following conditions: temperature, 25 °C; gauge length, 30 mm; crosshead speed, 100 mm $\text{min}^{-1}$. The initial cross section (23.75 $\text{mm}^2$) was used to calculate the tensile strength ($\sigma$) and the modulus ($E$). The tensile moduli were calculated from the increase in load detected between the elongations of 5% and 15%. Compression tests were carried out for all gels using samples of the same size (10 mm × 10 mm × 10 mm), also on the Shimadzu Autograph AGS-H (load cell 1 kN). The compression properties of all gels were obtained under the following conditions: compression speed, 0.5 mm/s; compression distance, 8 mm (80%), data rate, 0.1 s. The compressions between 1 and 1.7 mm were used to determine the compressive moduli.

## Results and Discussion

**Preparation of NC−OR Gels.** Co-cross-linked PNIPA hydrogels were prepared by the in-situ, free-radical polymerization of NIPA in the presence of both cross-linkers, clay and BIS, with concentrations *n* and *m*, as defined above, respectively, in aqueous media. The resulting hydrogels (NC*n*−OR*m* gels) were all uniform and exhibited no macroscopic phase separation or syneresis, regardless of *n* or *m*. The polymerization yields were almost 100% (>99.9%) in all cases. So, the resulting NC−OR gels had the same composition as the corresponding starting reaction solutions. This was confirmed by the thermogravimetric analysis of dried NC−OR gels. Also, since no free polymer (PNIPA) and no clay species were observed in the water used to swell the gels, it was concluded that all polymer chains and all of the clay were incorporated into the networks of the NC−OR gels. Furthermore, it was observed by TEM measurement for dried NC−OR gels, as described below, that the clay was exfoliated and molecularly dispersed throughout the sample in a manner similar to that in the dried NC gels.[14] Thus, it can be presumed that NC*n*−OR*m* gels consist of a combined network of NC*n* and OR*m* gels. In practice, different numbers of chemical cross-links, according to *m*, are incorporated into the organic/inorganic network architecture of NC*n* gels.

**Transparency of NC*n*−OR*m* Gels.** As previously reported,[14] the transparency of OR*m* gels shows a clear dependence on *m* (BIS concentration). OR*m* gels with low *m* values ($m < 3$) were highly transparent, while the transparency decreased rapidly with further increases in *m*, and at $m \geq 5$, the OR*m* gels became totally opaque, as shown in Figure 1 (OR*m* gels). This is due to the frozen structural heterogeneity, as reported by Shibayama,[23] which is caused by the microscopic aggregation of chemical cross-links (i.e., BIS units) during the synthesis of the gels. In other words, the heterogeneous distribution of BIS that occurs during the course of polymerization leads to decreased transparency (i.e., reflection of visible light) in the resulting hydrogel. On the other hand, NC*n* gels are generally transparent almost regardless of the clay concentration *n*, although the transmittance shows a slight minimum at around $n = 2$ and a slight and gradual decrease in the range of high *n* values. For NC*n*−OR*m* gels, it was observed that the transparency changed greatly depending on *n* and *m*, as follows.

**(a) NC1−OR*m* Gels.** The transmittances ($T$), at 600 nm, of NC1−OR*m* gels are shown in Figure 1, together with those of

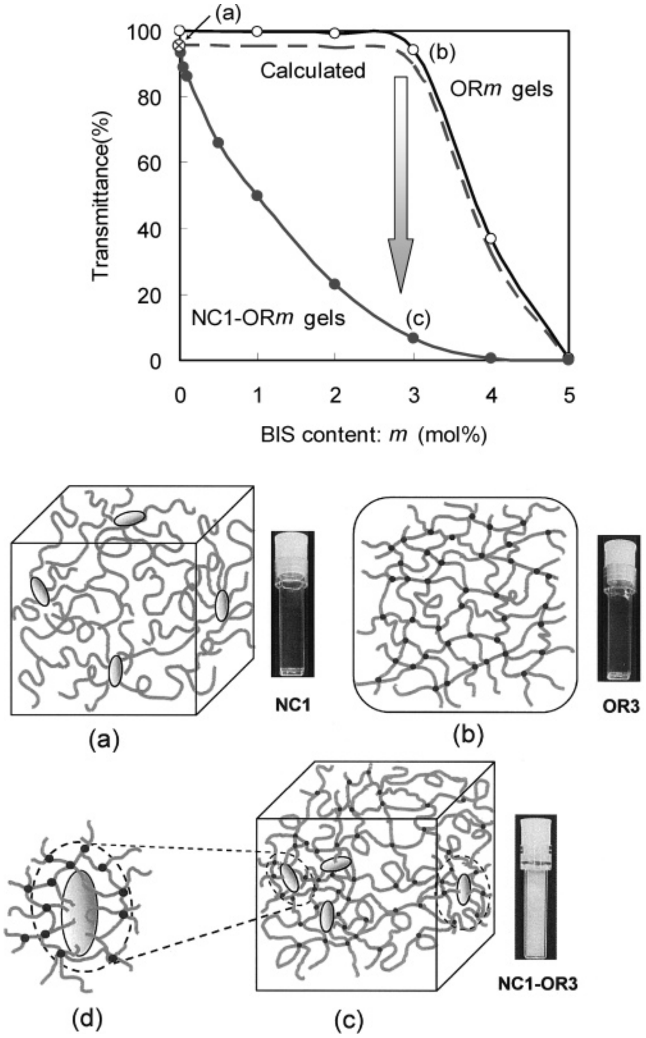

**Figure 1.** Transmittance changes in NC1−OR*m* gels with different BIS contents at 20 °C. The symbol "⊗" refers to the transmittance of NC1 gel. (a−c) Appearances and schematic representations of the structural models for NC1, OR3, and NC1−OR3 gels. (c, d) Chemical cross-links uniformly dispersed in the OR3 gel aggregate in the NC1−OR3 gel by the preferential distribution of BIS close to the clay platelets. Each microcomplex structure (d) is loosely aggregated in the system.

OR*m* gels and NC1 gel (⊗). Since the NC1 gel is transparent ($T = 96\%$) and OR*m* gels exhibit a clear-cut dependence on *m*, one can reasonably expect that the transparencies of NC1−OR*m* gels would exhibit the same dependence on *m* as that of OR*m* gels, starting at $T = 96\%$, as shown by the dotted line. However, the actual results for NC1−OR*m* gels differed greatly from those expected. That is, the transmittance rapidly decreased at low BIS concentrations ($m < 2$) and reached a very low value ($T = 6\%$) at $m = 3$, although the corresponding OR1 to OR3 gels were all transparent ($T = 100$ to $96\%$). These results indicate that the networks of NC1−OR*m* gels are not formed by the simple addition of the two corresponding homogeneous NC and OR gel networks but have a kind of microstructure with heterogeneities on the wavelength scale of visible light.

As shown in Figure 1, the transmittance of NC1−OR*m* gels started to decrease when a very small amount of BIS, such as $m = 0.01$, 0.05, or 0.1, was incorporated. Also, when comparing two types of hydrogels, e.g., the OR2 gel ($T = 100\%$) and the NC1−OR2 gel ($T = 23\%$), very different transmittances were observed, although the difference in composition was only a small amount of clay, 6.7 (0.68) wt % against PNIPA (total gel). From these results, it was deduced that the lower transparencies observed in NC1−OR*m* gels can be related to the specific combination of clay and BIS. That is, the PNIPA chains surrounding the clay platelets were predominantly cross-linked by BIS. Thus, the density of the chemical cross-links near the periphery of the clay particles was higher than average, while in the outer regions, farther away from the particles, it was lower. Here, the microstructure formed in the co-cross-linked network and responsible for the reduced transparency is termed the "microcomplex structure". A schematic representation of the microcomplex structure, consisting of exfoliated clay platelets and chemically cross-linked PNIPA chains surrounding the clay, is shown in Figure 1d. The density of the chemical cross-links in the microcomplex structure and the difference from that in the outer region should change depending on *m* and *n*, or, more correctly, on the ratio $m/n$. As readily expected, the difference in the density of the chemical cross-links should be very high when *n* is low and $m/n$ is high, as in NC1−OR3, and should diminish at high *n* and high *m*.

Considering the pronounced decrease in the transparency of the NC1−OR3 gel, the transparency might also be affected by a further concentration of chemical cross-links induced by the aggregation of microstructure units. By analogy with OR*m* gels with high *m*, where the microscopic aggregation of chemical cross-links occurs during the synthesis, thereby rendering the OR*m* gels totally opaque, it is considered that the microcomplex structures with fairly high chemical cross-link densities may aggregate with each other during synthesis, particularly at low *n* and high $m/n$. Concerning the aggregation of clay platelets, which is central to the microcomplex structures, we speculated that it may be useful to observe the clay dispersion morphology in dried gels by TEM. Since NC−OR gels contracted uniformly, maintaining a form similar to the original one as they dried, and each clay sheet was linked with neighboring clay sheets via a number of polymer chains, it was thought that the clay dispersion in the dried state may reflect that in the hydrogel state. As shown in Figure 2a, the clay platelets aggregated to some extent in a thin film of dried NC1−OR3 gel. Here, the clay was molecularly exfoliated, but the discrete clay platelets aggregated loosely and irregularly in the dried state, although, in the hydrogel state, the interclay distances will increase substantially upon swelling. The loose and irregular aggregation was also confirmed by X-ray diffraction measurements. No distinct diffraction peak was observed in the $2\theta$ range from 1.5° to 5° in the dried NC1−OR3 gel, a situation similar to that of the other NC gels,[18] which means that there is no regular stacking of clay platelets or of the clay/polymer intercalation in the dried NC1−OR3 gel, and, by analogy, in the nondried NC1−OR3 gel as well.

Schematic representations of the network structures as well as the appearances of the NC1, OR3, and NC1−OR3 gels are shown in parts a, b, and c of Figure 1, respectively. The high concentration of chemical cross-links in the microcomplex structure may be attributed to the existence of a preferential distribution of BIS to the immediate surroundings of the clay particles in the reaction solution. The mechanism of microcomplex structure formation will be discussed in a later section.

**(b) NC10−OR*m* Gels.** Provided that the formation of microcomplex structures and their loose aggregation are responsible for the abnormal decrease in transmittance, the effects should be very marked when *n* is low and *m* is fairly high, as in NC1−OR2 or −OR3 gels, because the difference in the chemical cross-link density between the microcomplex structure and the outer matrix region should be accentuated when the concentration of clay particles is low and the number of BIS

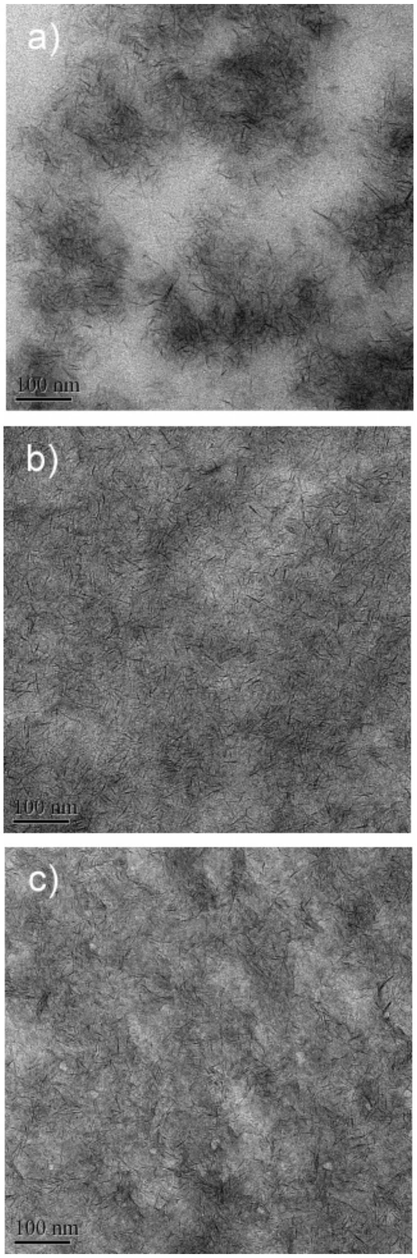

**Figure 2.** Transmission electron micrographs of dried (a) NC1−OR3, (b) NC5−OR1, and (c) NC10−OR5 gels at a magnification of 300 000.

units preferentially distributed to the vicinity of the clay particles is consequently large. This view is consistent with the results presented in the former section.

This implies that the decrease in transmittance would be reduced at higher *n* because, at constant *m*, the number of BIS molecules per clay particle decreases with increasing *n*. Also, when both *n* and *m* are high (and *m*/*n* is therefore not high), the transparency is minimal because a large number of microcomplex structures with a fairly low difference in chemical cross-link density from that of the surroundings are dispersed uniformly, without microscopic aggregation, throughout the system and may result in gels with a homogeneous distribution of chemical cross-links on the wavelength scale of visible light. The changes in the optical transmittance of NC−OR gels with high *n* values, on changing the *m* values, are shown in Figure 3 for NC10−OR*m* gels and compared with those of NC10 gel (⊗) and OR*m* gels. It was found that the change in transmittance with *m* differs from that expected from the simple summation of the values for the two individual types of network (dotted line). However, the deviations from the calculated line are in the opposite sense to that for NC1−OR*m* gels. That is, in the NC1 series, the transmittance decreased rapidly in the range of low BIS content (Figure 1), but in the NC10 series (Figure 3), the transmittance decreased monotonically but only by a small amount throughout the *m* range of 0−5, and the gel retained a high transmittance even at high *m* ($m = 5$, $m/n = 0.5$).

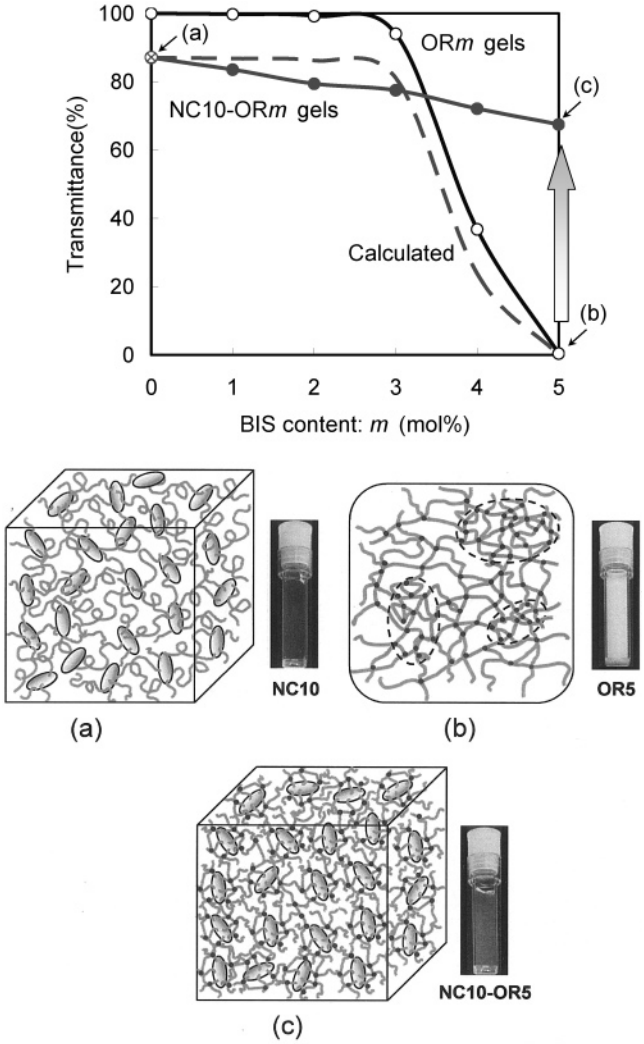

**Figure 3.** Transmittance changes in NC10−OR*m* gels with different BIS contents at 20 °C. The symbol "⊗" refers to the transmittance of NC10 gel. (a−c) Appearances and schematic representations of the structural models for NC10, OR5, and NC10−OR5 gels. The heterogeneous aggregation of chemical cross-links observed in the OR gels is depressed in the NC10−OR5 gel.

The changes in transmittance observed in NC10−OR*m* gels can also be explained by the formation of the same microcomplex structures, as follows. At low *m* ($m < 3$), only a slight and gradual decrease in transmittance was observed with increasing *m*, which is mainly due to the small number of BIS molecules per clay particle (e.g., $m/n = 0.1$ for the NC10−OR1 gel). At $m = 3$, the actual data crossed the calculated line. At high *m* ($m > 3$), the transmittances were higher than those calculated. For example, the NC10−OR5 gel (Figure 3c) exhibited a remarkably high transparency ($T = 68\%$), although the OR5 gel (Figure 3b) was opaque ($T = 0\%$). This means that the network heterogeneity observed in the OR5 gel, i.e., the heterogeneous aggregation of chemical cross-links, was suppressed by the presence of the clay. That is, the distribution of chemical cross-links in the NC10−OR5 gel was quite homogeneous. This is because a large number of microcomplex

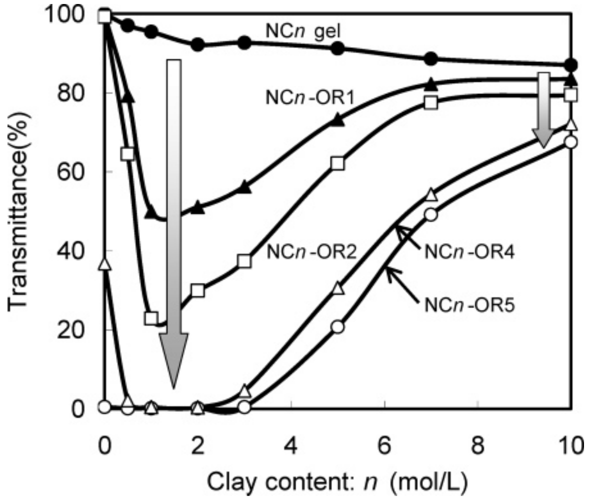

**Figure 4.** Effect of the clay content on the transmittance of NC and NC$n$−OR$m$ gels at 20 °C.

structures with a relatively low difference in the density of chemical cross-links ($m/n = 0.5$) from that of the matrix developed uniformly throughout the gel. The uniform dispersion of exfoliated clay platelets in dried NC$n$−OR$m$ gels with high $n$, such as $n = 5$ or 10, was confirmed by TEM observation, as shown in parts b and c of Figure 2 for the dried NC5−OR1 gel and the dried NC10−OR5 gel, respectively. It was observed that the clay was perfectly exfoliated and uniformly dispersed throughout the dried gels, particularly in the dried NC5−OR1 gel (Figure 2b). Schematic representations of the network structures as well as the appearances of the NC10, OR5, and NC10−OR5 gels are shown in parts a, b, and c of Figure 3, respectively.

**(c) NC*n*−OR*m* Gels.** In NC$n$−OR$m$ gels with moderate clay concentrations (e.g., NC5−OR$m$ gels), the changes in transparency were intermediate between those of NC1−OR$m$ and NC10−OR$m$. The overall tendencies in the transmittance change for NC$n$−OR$m$ gels produced by altering the $n$ (0−10) and the $m$ (1−5) values are summarized in Figure 4. Here, the effects of $n$ on the transmittance at various constant $m$ values are shown. At low $n$ (up to $n \sim 3$), the transmittance decreased markedly with increasing $m$, while decreasing less at high $n$ (e.g., $n = 10$). These results indicate that the incorporation of chemical cross-links into the organic/inorganic network accelerates the decrease in transparency when the clay concentration $n$ is low and that the decrease is more subdued when $n$ is high.

Figure 5 shows a schematic representation of the relationship between the distribution of clay particles and the chemical cross-linking units (BIS) for the cases in which (a) $m$ is constant and (b) $m/n$ is constant. In the case of (a), the total BIS content is the same, so the transparency increases with increasing $n$. At low $n$, the clay accelerates the aggregation of the chemical cross-links, but at high $n$, the clay improves the uniform dispersion of the chemical cross-links. In the case of (b), the number of BIS units per clay particle is fixed. Therefore, the transparency gradually decreases with increasing $n$ (from b-1 to b-2). However, with further increase in clay content, the system appears uniform on the wavelength scale of visible light, so the transmittance of the gel increases. These predicted behaviors were indeed observed in actual NC$n$−OR$m$ gels, as shown in Figure 5c. The dotted lines plotted for the same $m/n$ values (0.1, 0.5, and 1.0) all exhibit a minimum at the intermediate $m$. The selective distribution of chemical cross-links (BIS) in the periphery of the clay platelets was also consistent with the findings for the mechanical properties of NC−OR gels and the change in viscosity of the clay aqueous solution upon the addition of BIS, as explained in a later section.

**Mechanical Properties of NC*n*−OR*m* Gels.** As described in the Introduction, NC gels exhibit extraordinary toughness, with high elongations at break and controllable moduli and strengths, due to their unique organic/inorganic network structure. On the other hand, OR gels are fragile because their network structures have large numbers of randomly distributed chemical cross-links. What, precisely, are the mechanical properties of NC−OR gels? The mechanical properties of NC$n$−OR$m$ gels were investigated in terms of two deformation modes: elongation and compression.

**(1) Tensile Mechanical Properties.** From tensile tests on a consecutive series of NC−OR gels, it was found that, in general, NC$n$−OR$m$ gels fractured readily on elongation, exhibiting very low elongations at break and low strengths, very much like OR$m$ gels (Figure 6a−c). Typical strain−stress curves for NC5−OR$m$ gels with different $m$ values are shown in Figure 6d. In these experiements, the $m$ was varied over a wide range, but shown in the figure are data only for a small range of $m$ values, from 0.02 to 1. NC5−OR$m$ gels with higher $m$, such as NC5−OR2 or NC5−OR5 gels, were all weak and brittle, like the NC5−OR1 gel. The fact that NC−OR gels are, as a whole, fragile indicates that, by analogy with OR gels, the chemical cross-links may be a major factor determining their tensile properties. As shown in Figure 6d, the use of small amounts of BIS together with clay (e.g., $m = 0.02−0.3$) greatly decreased the strength and elongation at break of the gels compared with the mechanically tough NC5 gel, while their modulus increased. Consequently, NC5−OR$m$ gels with $m \geq 0.5$ exhibited pronounced brittleness and weakness, very much like OR$m$ gels with their inferior tensile properties. This fragility was also observed in other NC$n$−OR$m$ gels over a wide range of clay concentrations ($n = 1−10$). Therefore, it is concluded that the co-cross-linked networks of NC$n$−OR$m$ gels mostly contain well-dispersed chemical cross-links except at very low $m$ (<0.3 in the case of $n = 5$), judging from their response to tensile deformations.

The results described above are consistent with the existence of microcomplex structures in the co-cross-linked networks (Figures 1 and 3). That is, the chemical cross-links are well dispersed throughout the gel, except at very low $m$ (~0.1), where the networks of NC$n$−OR$m$ gels still contain flexible PNIPA chains in the outer (matrix) region due to the preferential concentration of chemical cross-links in the microcomplex structures.

With regard to the initial tensile modului of NC−OR gels, the moduli generally increased with increasing $m$, as readily expected from their composition (Figure 6d). However, an analysis of all data for NC$n$−OR$m$ gels revealed that the initial moduli show characteristic dependencies on $m$ and $n$. Changes in the initial modulus for various NC$n$−OR$m$ gels with different $m$ and $n$ values, together with those for OR$m$ gels, are summarized in Figure 7. Here, since the moduli of the network materials are basically proportional to the effective cross-link density,[24] the moduli of NC$n$-OR$m$ gels were initially estimated by the simple summation of the two moduli of the corresponding OR$m$ and NC$n$ gels; these calculated values are shown as dotted lines, while the observed moduli are shown as solid lines. A comparison of these pairs of data sets revealed that the actual moduli were mostly greater than those calculated. The discrepancies from the estimated values were very small for the NC1−OR$m$ gels but were very large for NC$n$−OR$m$ gels with high $n$ values. Also, at constant $n$, the discrepancies increased markedly with increasing $m$. Thus, NC$n$−OR$m$ gels with high $n$ and $m$,

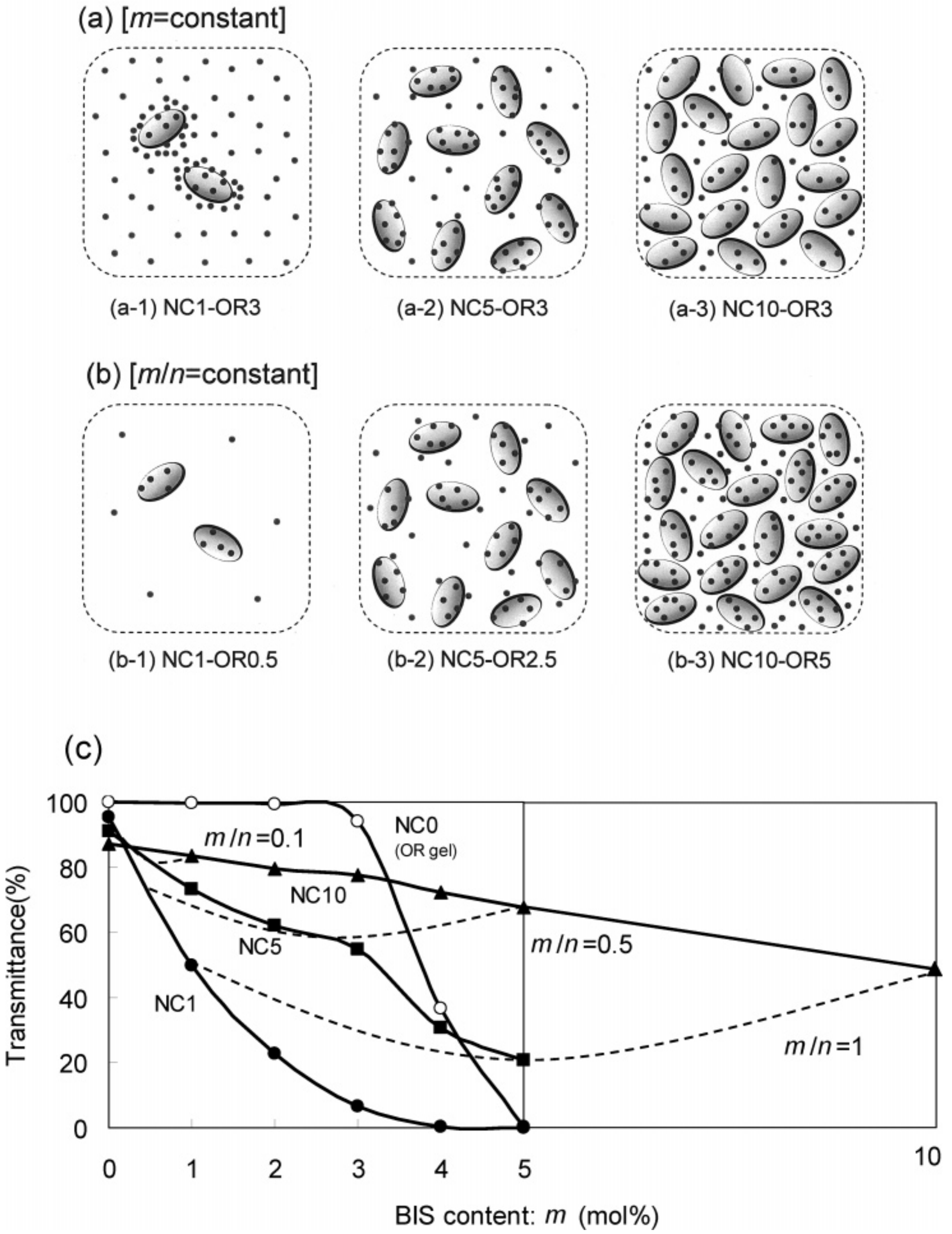

**Figure 5.** (a, b) Schematic representations of the distribution of the clay platelets and the chemical cross-linking points (BIS) in NC*n*−OR*m* gels. (c) Effect of the BIS content on the transmittance of OR*m* and NC*n*−OR*m* gels at 20 °C.

such as NC5−OR5 and NC10−OR5 gels, showed large differences between the observed moduli (an increase) and the calculated ones (Figure 7). On the other hand, in NC1−OR*m* gels, it was found that the actual moduli were mostly the same or slightly lower than those calculated.

Thus, remarkably high initial tensile moduli for NC*n*−OR*m* gels were achieved, compared with the calculated values (NC*n* gel + OR*m* gel), particularly for NC*n*−OR*m* with high *n* and high *m*. In contrast, NC*n*−OR*m* gels with low *n* or high *n* and low *m*, such as the NC1−OR∼5 and the NC5−OR∼0.5 gels, did not exhibit large increases in modulus. These changes in modulus are also explained by the proposed network model. The remarkably high moduli of NC*n*−OR*m* gels with high *n* and high *m* are ascribed to the very homogeneous distribution of chemical cross-links (Figure 3c), which was effective in increasing the modulus, whereas in the NC1−OR*m* gels, the moduli hardly increased, or were even lower than those calculated, because of the preferential distribution of chemical cross-links toward local sites (microcomplex structures), which caused the aggregation of chemical cross-links, thus rendering them ineffective in increasing the modulus (Figure 1c).

**(2) Compressive Mechanical Properties.** We will now consider the compressive mechanical properties of NC*n*−OR*m* gels. As reported previously, NC*n* gels are flexible and remarkably tough (Figure 8a). On the other hand, OR*m* gels are, in general, readily fractured asunder on compression by hand, almost regardless of *m* (Figure 8b). So, since a large number of chemical cross-links may act as the predominant factor in the deformation induced by an external force, we suggest that the compressive properties of NC*n*−OR*m* gels in general change in a manner similar to the tensile behavior described above. That is, the compressive strength of NC*n*−OR*m* gels closely approaches that of OR*m* gels with increasing *m*. So, for example, it was predicted that NC*n*−OR1 gels would suffer brittle fracturing in compression tests, like the OR1 gel. However, it was found that the actual data were quite different from the predictions, as shown in Figure 8c. In the following parapgraphs, the compressive mechanical properties of NC*n*−

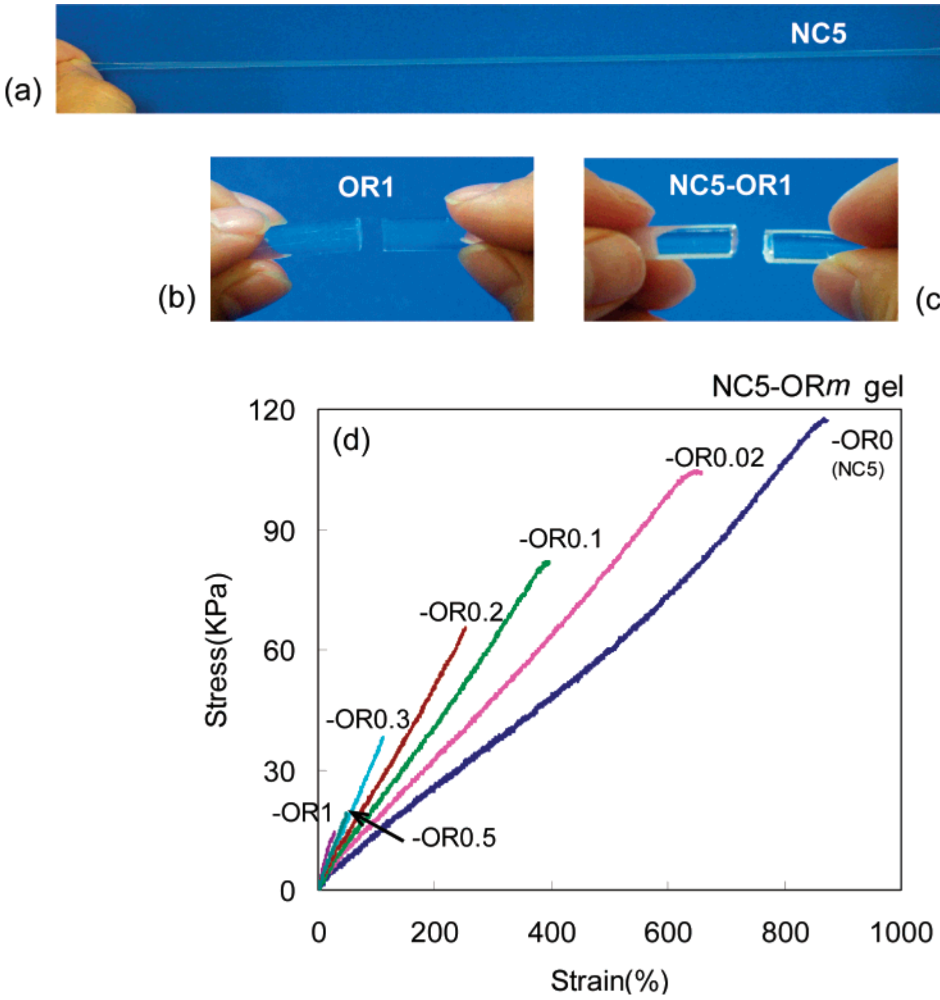

**Figure 6.** (a−c) Differences in the tensile mechanical behavior of (a) NC5, (b) OR1, and (c) NC5−OR1 gels. (d) Stress−strain curves for NC5−ORm gels with different organic cross-linker contents (*m* = 0−1).

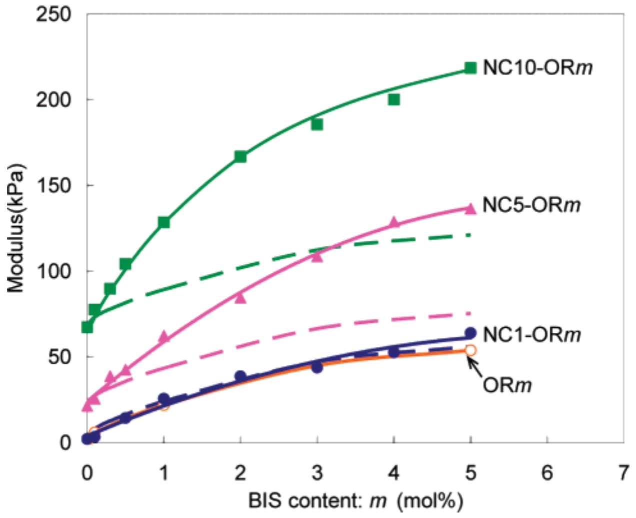

**Figure 7.** Effect of the organic cross-linker content (*m*) on the tensile moduli of OR*m* and NC*n*−OR*m* gels. The dashed lines are the values calculated by the simple summation of the two moduli of the corresponding OR*m* and NC*n* gels.

OR*m* gels are described separately for two groups, gels with low *m* (≤1) and gels with high *m* (e.g., *m* = 2−5), in terms of the different effects of the chemical cross-links on the compressive properties.

**(a) NC*n*−OR*m* Gels (*m* ≤ 1).** As shown in Figure 8c, NC5−OR1 gel exhibited a tough compressive behavior similar to that of NC5 gel, but different from that of the fragile OR1 gel. The compressive stress−strain curves (up to 80% compression) of NC5−OR*m* gels with different *m* values are shown in Figure 8d (thick, solid lines), together with that of the NC5 (i.e., NC5−OR0) gel (in blue) and the OR1 gel (in orange). Here, the OR1 gel fractured at a strain of about 70% and low compressive strength (0.7 MPa). The NC5 (= NC5−OR0) gel showed a relatively low modulus, like the OR1 gel, but had not yet fractured at 90% compression and 6.6 MPa stress, although the stress required to achieve 80% compression was quite low (0.7 MPa). In contrast, NC5−OR*m* gels (*m* ≤ 1) generally had higher rigidity (modulus) and could withstand deformations in excess of 80%. Figure 8d shows that the compressive strengths of NC5−OR*m* gels at 80% strain were increased to a remarkable extent by only small increases in *m*, e.g., 2.8 MPa (*m* = 0.02), 4.5 MPa (*m* = 0.3), and 5.2 MPa (*m* = 1). The compressive strengths (at 80% strain) were equal to or higher than those of NC*n* gels with very high clay concentrations, e.g., NC15 (2.9 MPa) and NC20 (4.9 MPa).[16] This is somewhat astonishing because it means that the excellent compressive properties of the original NC gels can be improved even further by the incorporation of quite small amounts of chemical cross-links, and the resulting NC−OR gels will readily show remarkable improvements in compressive strength and modulus while retaining their high compressive deformability. The compressive strengths at 80% strain were comparable to the highest values reported for double-network hydrogels.[25]

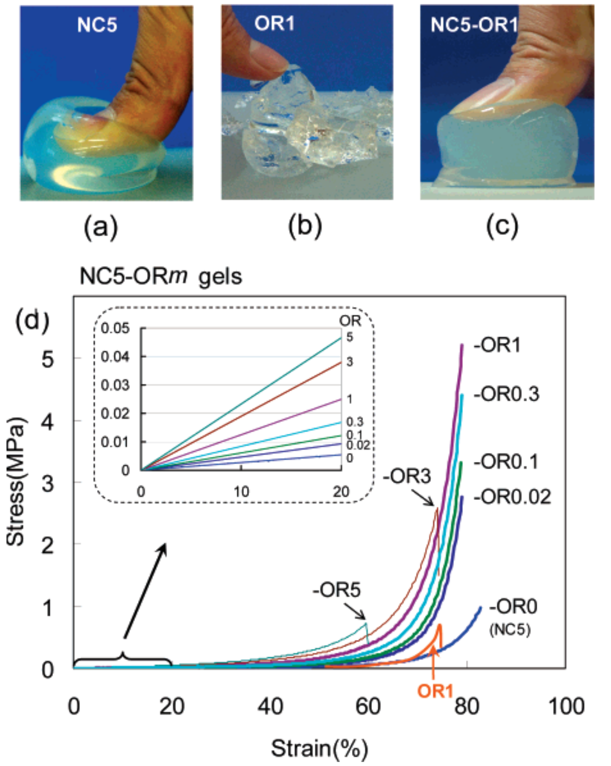

**Figure 8.** (a−c) Differences in the compression behavior of (a) NC5, (b) OR1, and (c) NC5−OR1 gels. (d) Stress−strain curves for NC5−OR$m$ gels with different organic cross-linker contents ($m$ = 0−5). NC5−OR$m$ gels with $m$ = 0−1 did not fracture when compressed up to 80%.

As for other NC$n$−OR$m$ gels (e.g., NC10−OR$m$, NC2−OR$m$), the NC10−OR$m$ gels ($m \leq 1$) exhibited the same behavior as the NC5−OR$m$ gels; i.e., they did not fracture. The strengths (at 80% strain) of the NC10−OR$m$ gels were the same as or slightly lower than those of the corresponding NC5−OR$m$ gels, while their initial compressive moduli were higher than (almost double) those of the NC5−OR$m$ gels. On the other hand, the NC2−OR$m$ gels ($m \leq 1$) generally showed very low strengths, e.g., 0.45 MPa ($m$ = 0.1) and 0.91 MPa ($m$ = 0.5), compared with the NC5−OR$m$ and the NC10−OR$m$ gels. Thus, it was concluded that NC$n$−OR$m$ gels with high $n$ (e.g., $n$ = 5, 10) and low $m$ ($\leq$1) exhibit greatly improved compressive properties but that such improvements are very small at low $n$ ($n \leq 2$).

The compressive behavior of NC$n$−OR$m$ gels can also be explained by the network model proposed. In the case of high $n$ and low $m$ (e.g., $n \geq 5$, $m \leq 1$), large numbers of microcomplex structures are formed uniformly throughout the gel, which was confirmed by TEM observation for the NC5−OR1 gel (Figure 2b), whereas the PNIPA chains within the microcomplex structures form only light chemical cross-links because of the limited number of BIS units per clay particle (i.e., small $m/n$ value). Furthermore, the PNIPA chains in the outer region are also cross-linked to a lesser extent, probably because most of the BIS is preferentially distributed to the microcomplex structures. Consequently, NC$n$−OR$m$ gels with slightly inhomogeneous networks consisting of loosely cross-linked PNIPA chains in the microcomplex structure and very lightly cross-linked flexible PNIPA chains in the outer region can withstand compressive strains, while the initial moduli are increased significantly because the chemical cross-links existing within the microcomplex structures are spread quite uniformly throughout the gel, accompanied by the uniform dispersion of clay platelets. On the other hand, at low $n$, since the number of BIS units per clay particle ($\propto m/n$) is high and there are also appreciable spaces throughout the outer region, the excess BIS should form a greater proportion of chemical cross-links in the outer region, as in OR gels. Thus, NC$n$−OR$m$ gels with low $n$ tend to undergo brittle fracturing, in analogy to OR$m$ gels.

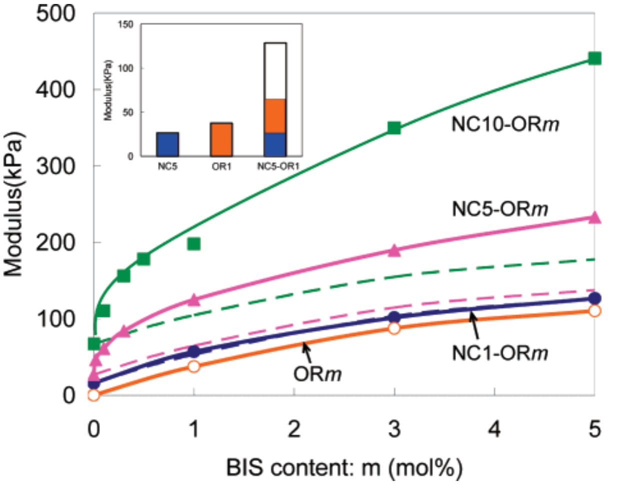

**Figure 9.** Effect of the organic cross-linker content ($m$) on the compression moduli of NC$n$−OR$m$ and OR$m$ gels. The dashed lines are the values calculated by the simple summation of the two moduli of the corresponding OR$m$ and NC$n$ gels.

**(b) NC$n$−OR$m$ Gels ($m \geq 2$).** Figure 8d also shows the stress−strain curves (thin, solid lines) for NC5−OR$m$ gels with high $m$ (= 3, 5). It was found that NC5−OR$m$ gels with high $m$ were brittle and that their compressive behavior approached that of OR$m$ gels with increasing $m$. This behavior is totally distinct from that of gels with low $m$ values ($m \leq 1$) described above. For other $n$ values (= 10, 2), the NC10−OR$m$ gels ($m \geq 2$) exhibit a slightly higher strength than the same strain at break as the NC5−OR$m$ gels, whereas the NC2−OR$m$ gels ($m \geq 2$) generally showed very low strength and low strain at break. Thus, all NC$n$−OR$m$ gels with $m \geq 2$ fractured under compression until 80% strain regardless of $n$ ($n$ = 1−10), and the ultimate strength (at break) decreased steeply with increasing $m$. The strain at break, which decreased with increasing $m$, was slightly greater than that of the corresponding OR$m$ gels. The brittleness of NC$n$−OR$m$ gels with high $m$ can also be explained by the network model proposed. For example, the NC2−OR5 gel ($m/n$ = 2.5) was brittle because the excess BIS formed chemical cross-links in the outer region; the NC10−OR5 gel ($m/n$ = 0.5) was brittle because a homogeneous distribution of chemical cross-links was established in the gel.

**(c) Initial Compressive Moduli of NC$n$−OR$m$ Gels.** Abnormal increases in the initial compressive moduli were also observed in NC$n$−OR$m$ gels, particularly in those with high $n$ and high $m$, in analogy to the tensile moduli (Figure 7). As a typical example, the initial compressive moduli of NC5, OR1, and NC5−OR1 gels are shown in the inset of Figure 9. The modulus of the NC5−OR1 gel is much larger than the sum of those of the NC5 and OR1 gels. Such abnormal increases were observed across the entire series of NC$n$−OR$m$ gels ($n$ = 1, 5, 10: $m$ = 1−5), particularly at high $n$, as shown in Figure 9. Here, the dashed lines represent the calculated values obtained by the simple summation of the two moduli of the corresponding OR$m$ and NC$n$ gels. The actual moduli (solid lines) at high $n$ were much larger than those calculated. The increases in modulus were almost proportional to $m$ in the range of $m \geq 1$, and the slopes of the moduli's dependence on $m$ increased with increasing $n$. This indicates that the chemical cross-links

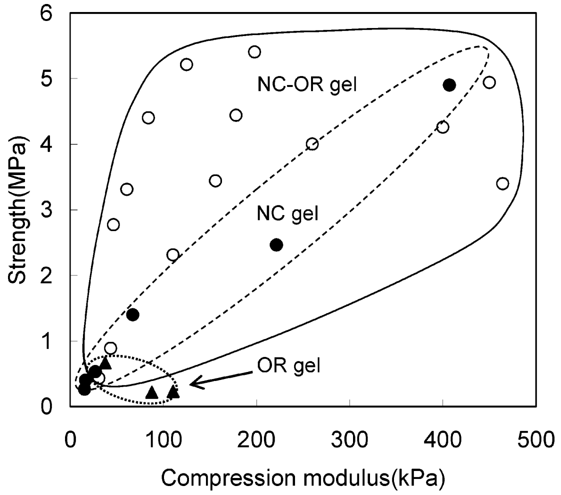

**Figure 10.** Correlation between the compression strength and the modulus, which are controllable in NC*n*, OR*m*, and NC*n*−OR*m* gels by altering the *n* (0−10) and *m* (0−5). The modulus−strength relationship can be controlled within each rounded area of the graph. Here, the strengths for the NC and NC−OR gels are at 80% compression (without fracture), whereas the strengths for the OR gels are at their maximum at break.

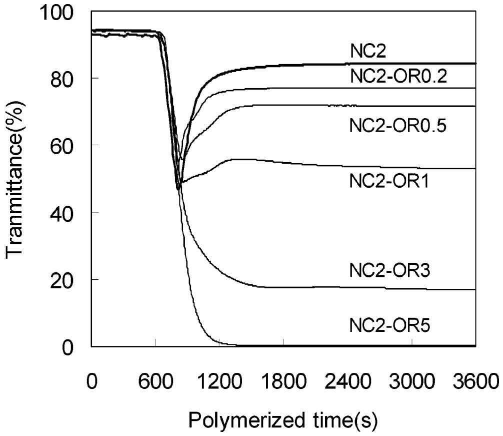

**Figure 11.** Changes in optical transparency during the polymerization of NC2 and NC2−OR*m* gels.

incorporated into NC*n*−OR*m* gels are so well dispersed that they effectively increase the compressive modulus and that their cross-linking efficiency increases with increasing *n*. At low *n* (e.g., $n = 1$), no abnormal increase was observed, but the modulus was almost the same as the sum of the moduli of the corresponding NC*n* and OR*m* gels. This tendency was the same as that observed for the initial tensile moduli.

In Figure 10, the correlations between the initial compressive moduli and the compressive strengths are summarized for the three types of PNIPA hydrogels studied: OR, NC, and NC−OR. In the figure, *n* and *m* were altered within the range of 0−10 and 0−5, respectively, for the NC*n*, OR*m*, and NC*n*−OR*m* gels. Here, the strengths for the NC*n* and NC*n*−OR*m* gels correspond to 80% compression without fracture (NC*n*−OR*m* gels which fractured before reaching 80% compression were not included), and the strengths for OR gels correspond to the fracture point. The conventional OR gels were always weak and brittle, readily rupturing under compression by finger pressure. So, in the correlation, only a small area (the rounded OR area of the graph) was covered. On the other hand, mechanically tough PNIPA hydrogel was successfully made for the first time by creating a new type of nanocomposite gel (NC gel) with a unique organic (PNIPA)/inorganic (clay) network structure. By altering the clay concentration, the compressive strength and initial modulus could be controlled over a wide range, as shown in Figure 10 (NC gels). All NC gels withstood a large compressive deformation of more than 80%. However, since the modulus and strength changed monotonically, in a linear fashion, with the clay concentration, a rather small region in the correlation was covered by the NC gels. In the present study, it was revealed that the strength−modulus correlation of the PNIPA hydrogel was considerably enhanced in NC−OR gels (Figure 10). Here, the combination of high strength and low modulus, which is usually a difficult and much sought-after requirement in materials design, was accomplished as well as the combination of high strength and high modulus.

**Formation of Microcomplex Structures.** NC−OR gels contain two types of cross-links in the PNIPA chains: chemical cross-links formed by the BIS units and physical cross-links to the clay particles. When the clay concentration is sufficiently high to form an organic/inorganic network ($n \geq 1$), the network of an NC−OR gel consists of the chemical cross-links incorporated into the organic/inorganic network architecture. From the characteristic changes in the optical and mechanical properties of NC−OR gels, it was concluded that the incorporation of chemical cross-links is not perfectly uniform and not the same as in OR gels but that microcomplex structures, consisting of clay platelets and PNIPA chains with a relatively high chemical cross-link density, are formed. With regard to the mechanism of microcomplex structure formation, it is proposed that chemical cross-links between PNIPA chains are formed predominantly in the vicinity of the clay platelets during NC−OR gel synthesis. The density of the chemical cross-links in the microcomplex structures naturally varies depending on the values of *n* and *m*, although the cross-link density in the microcomplex structures is always somewhat higher than that in the outer regions.

The enhanced formation of chemical cross-links in the microcomplex structures may derive from the preferential distribution of BIS to the periphery of the clay platelets in the initial reaction solution. This hypothesis was confirmed by measuring the changes in viscosity of aqueous clay suspensions (i.e., the time dependence of the viscosity) on adding BIS and NIPA. As reported previously,[18] the viscosity of aqueous clay suspensions gradually increases with retention time. This is because exfoliated clay platelets, whose surfaces and edges carry negative and positive charges, respectively, tend to form a so-called house-of-cards structure through ionic interactions. In Table 1, the effects of BIS and NIPA on the viscosity of an aqueous clay suspension ($C_{\text{clay}} = 4$ wt %) are shown. The increase in viscosity was depressed appreciably by the addition of either BIS or NIPA, and the magnitude of the decrease in viscosity was greater with BIS than with NIPA, when compared on both equi-molar and equi-amide-group bases. These results indicate that clay platelets are more effectively surrounded by BIS than by NIPA, probably due to interactions between the ionic clay and the dipolar BIS molecules. Thus, the chemical cross-linking of PNIPA chains took place predominantly in the surroundings of the clay platelets to form microcomplex structures with relatively high chemical cross-link densities.

The formation of microcomplex structures may also be related to the unique formation mechanism of NC gels. As previously reported,[18] the transmittance showed a remarkable change in the early stage of the in-situ polymerization of NC gels, particularly at low *n*, as in NC2 (Figure 11). The unusual decrease in transparency corresponded to the formation of clay−brush particles, which were formed due to the predominant

**Table 1. Viscosity Change Induced by the Introduction of BIS or NIPA into the Clay Solution**

| additives | none | BIS | | | | NIPA | | |
|---|---|---|---|---|---|---|---|---|
| concn ($10^{-2}$ mol per L of $H_2O$) | (clay solution) | 1 | 2 | 5 | 7 | 2 | 5 | 7 |
| viscosity (mPa·s)[a] | 506 | 409 | 316 | 233 | 225 | 480 | 430 | 269 |

[a] All viscosities were measured 60 min after preparation.

initiation at the clay surface. In the present study, the addition of a small amount of BIS to the reaction solution, as shown in Figure 11, did not induce the recovery of the transmittance as much as in the NC2 gel after it reached its minimum value. This may indicate that clay−brush particles were formed in a manner similar to the way they were formed in the original NC2 gel (OR0), but with increasing *m*, highly dense PNIPA chains were fixed in the clay−brush particles via chemical cross-links due to the reaction with BIS. With further increases in *m*, more densely packed chemical cross-links formed in the immediate surroundings of the clay particles, subsequently accelerating the loose aggregation of the resulting clay−brush particles. Hence, the transmittance continued to decrease to zero.

## Conclusion

Co-cross-linked PNIPA hydrogels were prepared by in-situ free-radical polymerization of NIPA in aqueous solutions containing two types of cross-linker: an organic cross-linker (BIS) and an inorganic cross-linker (clay). The resulting hydrogels (NC−OR gels) were investigated in terms of their optical properties and their tensile and compressive mechanical properties. The following results were found.

(1) The obtained NC*n*−OR*m* gels were uniform hydrogels regardless of the concentration of clay (*n*) and BIS (*m*) and, in all cases, completely lacked macroscopic phase separation or syneresis. The compositions of the NC*n*−OR*m* gels were the same as those of the corresponding starting solutions. NC−OR gels consist of combined networks of NC*n* and OR*m* gels. That is, different numbers of chemical cross-links, determined by the value of *m*, are incorporated into the organic (PNIPA)/inorganic (clay) network structures of NC*n* gels.

(2) The transparencies of NC*n*−OR*m* gels changed considerably according to the values of *n* and *m* and were generally different from the sum of the transparencies of the corresponding NC*n* and OR*m* gels. At low *n* (e.g., $n = 1$), NC1−OR*m* gels exhibited steep drops in optical transmittance with small increases in *m*, and at $m = 3$ (NC1−OR3), the gel became opaque although both the NC1 gel and the OR3 gel were transparent ($T > 90\%$). In the case of high *n* (e.g., $n = 10$), the transmittances of NC10−OR*m* gels slowly decreased with increasing *m*, and consequently, the NC10−OR5 gel still retained a fairly high transparency ($T = 68\%$), although the NC10 and the OR5 gels were transparent and opaque, respectively.

(3) In the tensile tests, NC*n*−OR*m* gels generally proved to be very weak and brittle, like OR*m* gels, almost regardless of *n* or *m*. This indicates that the chemical cross-links dispersed in a co-cross-linked network are a major factor in determining the tensile properties of NC−OR gels. With regard to the initial tensile moduli, large increases compared to the sum of the values of the corresponding NC*n* and OR*m* gels were observed, particularly in NC*n*−OR*m* gels with high *n* and *m*. The abnormal increases in the initial tensile moduli indicate that the chemical cross-links in NC−OR gels are dispersed quite well throughout the gel, acting as effective cross-links which increase the modulus to levels above those of OR gels.

(4) In the compressive mechanical tests, NC*n*−OR*m* gels exhibited two distinct properties depending on *m*. For $m \leq 1$, large improvements in compressive strength were achieved, and the samples did not fracture below 80% strain. These improved properties were observed to be especially large in NC*n*−OR*m* gels with high *n*, e.g., $n = 5$ or 10. In the case of $m > 1$, the NC*n*−OR*m* gels tended to undergo brittle fracturing at ultimate strains of less than 80%, almost regardless of *n*. With regard to the initial compressive moduli, large increases above the estimated values were observed, in analogy to the initial tensile moduli. This tendency was very marked in NC*n*−OR*m* gels with high *n* and *m*. As a result, it was found that, in terms of the correlation between strength and initial modulus, NC−OR gels can boost the compressive properties of PNIPA hydrogels to a new level.

(5) All of the characteristic optical and mechanical properties observed in the present study indicate that a kind of microstructure, referred to as the “microcomplex structure” and consisting of exfoliated clay platelets with enhanced densities of chemically cross-linked PNIPA chains, is formed in all NC−OR gels. So, in NC*n*−OR*m* gels, the distribution of the chemical cross-links incorporated into the organic/inorganic network architecture varied greatly, from heterogeneous to homogeneous, depending strongly on the values of both *n* and *m*. For example, at high *n* (e.g., NC10−OR*m* gels), a large number of (clay platelet-centered) microcomplex structures were well dispersed throughout the system, and the difference in the chemical cross-link density between the microcomplex structures and the outer region was fairly small due to the low *m*/*n*. This means that the chemical cross-links were homogeneously distributed throughout the gel, almost regardless of *m*. Thus, for example, the NC10−OR1 and the NC5−OR1 gels were simultaneously very tough, very strong (superior compressive property), and highly transparent, but also very brittle (inferior tensile property), whereas the NC10−OR5 gel exhibited quite high transparency, although the OR5 gel was opaque. On the other hand, at low *n* (e.g., NC1−OR*m* gels), a heterogeneous distribution of chemical cross-links and a loose aggregation occurred due to the low number of microcomplex structures with highly dense chemical cross-links (high *m*/*n*). This structure causes a large decrease in transparency and mainly brittleness, i.e., inferior tensile and compressive strength.

(6) It was hypothesized that microcomplex structures may be formed due to the preferential distribution of BIS to the immediate vicinity of the clay platelets in the reaction solution. This was confirmed by the reduced increase in the viscosity of aqueous clay solutions with retention time. The formation of microcomplex structures may also be related to the formation of clay-brush particles during NC−OR gel synthesis.

**Acknowledgment.** We thank Mr. E. Elliott for his technical assistance and Ms. J. Sano and Mr. S. Matsumoto for the TEM measurements. This work was partially supported by NEDO, Japan.

## References and Notes

(1) Heskins, M.; Guillet, J. E. *J. Macromol. Sci., Chem.* **1968**, *8*, 1441−1455.

(2) Bae, Y. H.; Okano, T.; Kim, S. W. *J. Polym. Sci., Part B: Polym. Phys.* **1990**, *28*, 923−936.

(3) (a) Hirokawa, Y.; Tanaka, T. *J. Chem. Phys.* **1984**, *81*, 6379−6380. (b) Hirotsu, S.; Hirokawa, Y.; Tanaka, T. *J. Chem. Phys.* **1987**, *87*, 1392−1395. (c) Matsuo, E. S.; Tanaka, T. *J. Chem. Phys.* **1988**, *89*, 1695−1703.

(4) (a) Li, Y.; Tanaka, T. *J. Chem. Phys.* **1989**, *90*, 5161−5166. (b) Otake, K.; Inomata, H.; Konno, M.; Saito, S. *Macromolecules* **1990**, *23*, 283−289. (c) Shibayama, M.; Tanaka, T. *J. Chem. Phys.* **1992**, *97*, 6829−6841.

(5) (a) Suzuki, A.; Tanaka, T. *Nature (London)* **1990**, *346*, 345−347. (b) Inomata, H.; Goto, S.; Otake, K.; Saito, S. *Langmuir* **1992**, *8*, 687−690. (c) Takigawa, T.; Araki, H.; Takahashi, K.; Masuda, T. *J. Chem. Phys.* **2000**, *113*, 7640−7645.

(6) Imai, Y.; Yoshida, N.; Naka, K.; Chujo, Y. *Polym. J.* **1999**, *31*, 258−262.

(7) Messersmith, P. B.; Znidarsich, F. *Mater. Res. Soc. Symp. Proc.* **1997**, *457*, 507−512.

(8) Liang, L.; Liu, J.; Gong, X. *Langmuir* **2000**, *16*, 9895−9899.

(9) Yoshida, R.; Uchida, K.; Kaneko, Y.; Sakai, K.; Kikuchi, A.; Sakurai, Y.; Okano, T. *Nature (London)* **1995**, *374*, 240−242.

(10) (a) Okajima, T.; Harada, I.; Nishio, K.; Hirotsu, S. *Jpn. J. Appl. Phys.* **2000**, *39*, L875−L877. (b) Zhang, X.-Z.; Zhuo, R.-X. *Langmuir* **2001**, *17*, 12−16. (c) Serizawa, T.; Wakita, K.; Akashi, M. *Macromolecules* **2002**, *35*, 10−12.

(11) Huglin, M. B.; Liu, Y.; Velada, J. L. *Polymer* **1997**, *38*, 5785−5791.

(12) (a) Yoshida, R.; Takahashi, T. *J. Am. Chem. Soc.* **1996**, *118*, 5134−5135. (b) Makino, K.; Hiyoshi, J.; Ohshima, H. *Colloids Surf., B* **2001**, *20*, 341−346.

(13) Haraguchi, K.; Takehisa, T. *Adv. Mater.* **2002**, *14*, 1120−1124.

(14) Haraguchi, K.; Takehisa, T.; Fan, S. *Macromolecules* **2002**, *35*, 10162−10171.

(15) Haraguchi, K.; Li, H-.J. *Angew. Chem., Int. Ed.* **2005**, *44*, 6500−6504.

(16) Haraguchi, K.; Li, H-.J. *Macromolecules* **2006**, *39*, 1898−1905.

(17) Haraguchi, K.; Farnworth, R.; Ohbayashi, A.; Takehisa, T. *Macromolecules* **2003**, *36*, 5732−5741.

(18) Haraguchi, K.; Li, H-.J.; Matsuda, K.; Takehisa, T.; Elliot, E. *Macromolecules* **2005**, *38*, 3482−3490.

(19) Shibayama, M.; Karino, T.; Miyazaki, S.; Okabe, S.; Takehisa, T.; Haraguchi, K. *Macromolecules* **2005**, *38*, 10772−10781.

(20) Miyazaki, S.; Karino, T.; Endo, H.; Haraguchi, K.; Shibayama, M. *Macromolecules* **2006**, *39*, 8112−8120.

(21) Bandi, S.; Bell, M.; Schiraldi, D. A. *Macromolecules* **2005**, *38*, 9216−9220; *Science* **2005**, *310*, 407.

(22) Katti, A.; Shimpi, N.; Roy, S.; Lu, H.; Fabrizio, E. F.; Dass, A.; Capadona, L. A.; Leventis, N. *Chem. Mater.* **2006**, *18*, 285−296.

(23) Shibyama, M. *Macromol. Chem. Phys.* **1998**, *199*, 1−30.

(24) Tobolsky, A. V.; Carlson, D. W.; Indicto, N. *J. Polym. Sci.* **1961**, *54*, 175−192.

(25) Gong, J. P.; Katsuyama, Y.; Kurokawa, Y.; Osada, Y. *Adv. Mater.* **2003**, *15*, 1155−1158.

MA070695P